

Constraint density functional calculations for multiplets in a ligand-field applied to Fe-phthalocyanine

Kohji Nakamura,* Yukie Kitaoka, Toru Akiyama, and Tomonori Ito
Department of Physics Engineering, Mie University, Tsu, Mie 514-8507, Japan

M. Weinert

Department of Physics, University of Wisconsin-Milwaukee, Milwaukee, Wisconsin 53201, USA

A. J. Freeman

Department of Physics and Astronomy, Northwestern University, Evanston, Illinois 60208, USA
 (Received 13 September 2011; revised manuscript received 17 May 2012; published 18 June 2012)

Multiplets in a ligand field are treated within total-energy density-functional calculations by imposing density-matrix constraints on the d -orbital occupation numbers consistent with the local site and state symmetries. We demonstrate the utility of this approach for the case of isolated Fe phthalocyanine (FePc) molecules with overall D_{4h} symmetry: We find three stationary states of 3E_g , ${}^3A_{2g}$, and ${}^3B_{2g}$ symmetries of the Fe^{2+} ion, and total-energy calculations clearly demonstrate that the ground state is ${}^3A_{2g}$. By contrast, a columnar stacking of the FePc molecules (α -FePc) is found to change the ground state to 3E_g due to hybridization between adjacent molecules.

DOI: [10.1103/PhysRevB.85.235129](https://doi.org/10.1103/PhysRevB.85.235129)

PACS number(s): 71.15.Nc, 31.15.es, 75.50.Xx

I. INTRODUCTION

State-of-the-art *ab initio* electronic structure calculations based on density-functional theory (DFT) have been recognized as a powerful tool to explore the ground-state electronic structure. However, there are systems, such as transition-metal-based complexes and molecules, where the multiplet structure is essential for understanding the electronic structure. Because of the inherent multideterminant nature of the general atomic multiplet problem,¹ a general solution remains a challenging issue. Even in the presence of the lower symmetry caused by a ligand (or crystal) field, which may lift the atomic multiplet degeneracies, DFT calculations often cannot adequately treat the experimentally observed multiplet structures and thus fail to find the *true* ground state or the *lowest* state within a given ligand (or crystal) symmetry. This difficulty is intrinsically related to the fact that the charge (and spin) density belongs to the completely symmetric representation of a group, but the various multiplets (and their orbital occupations) transform according to *different* irreducible representations; i.e., the symmetry of the charge (spin) densities is *not* sufficient to distinguish among different multiplets since all the multiplets generate densities of the *same* symmetry. In order to overcome such difficulties, it is desirable to find an approach within DFT [local-density approximation or generalized gradient approximation (GGA)] calculations to find the lowest state of a given symmetry.

Proposed approaches for calculating multiplet energies in a ligand field include, for example, combining the DFT single-particle wave functions and configuration interaction (CI).^{2,3} Such CI calculations, however, are already outside of a DFT scheme depending on the charge and spin densities and are computationally expensive because of the need to construct appropriate (and/or enormous) multi-Slater determinants. Alternatively, in the present paper, we propose a simple DFT approach to treat multiplets in a ligand field,

consistent with the overall symmetry and the symmetry of the individual state, by imposing a density-matrix constraint to control the occupation numbers of electrons in, for example, the d orbitals. To illustrate our approach, we search for the ground-state multiplet for Fe phthalocyanine (FePc), a material with technological and biological applications.⁴

II. STRUCTURE OF Fe PHTHALOCYANINE

An isolated molecule of FePc has the simple planar structure shown in Fig. 1(a), where the Fe^{2+} (d^6) ion located at the center of the molecule has D_{4h} site symmetry. In condensed form, it shows two polymorphs: a metastable α form found in polycrystalline powders or in thin films with ferromagnetic order below 10 K⁵⁻⁹ and a stable paramagnetic β form¹⁰⁻¹³ obtained by sublimation growth as a single crystal or by heating α -FePc at 350°C. In both forms, the ligand field splits the d states into three singlets (d_{xy} , d_{z^2} , and $d_{x^2-y^2}$) and one doublet (d_{xz+yz}). Ignoring the high-lying $d_{x^2-y^2}$ state that bonds to the four outer N ions, three spin-triplet multiplets— 3E_g ($d_{xy}^2 d_{z^2}^1 d_{xz+yz}^3$), ${}^3B_{2g}$ ($d_{xy}^1 d_{z^2}^1 d_{xz+yz}^4$), and ${}^3A_{2g}$ ($d_{xy}^2 d_{z^2}^2 d_{xz+yz}^2$)—may be constructed, each of which generates a charge and spin density of D_{4h} symmetry.

Despite extensive experimental and theoretical investigations spanning decades, which multiplet is the ground state is still debated: Magnetic anisotropy experiments^{12,15} originally assigned the 3E_g multiplet as the ground state, but later magnetic susceptibility and magnetic circular dichroism experiments^{13,14} favored ground states of either ${}^3B_{2g}$ or ${}^3A_{2g}$ symmetry. (There is, however, general consensus that the ground state has $S = 1$.) Meanwhile, recent Mössbauer spectroscopy and x-ray magnetic circular dichroism (XMCD) experiments^{8,9} for α -FePc found a 3E_g ground state with a large orbital moment of 0.53 μ_B and a large hyperfine field of 66.2 T that is parallel to the magnetic moment.⁸ Magnetization

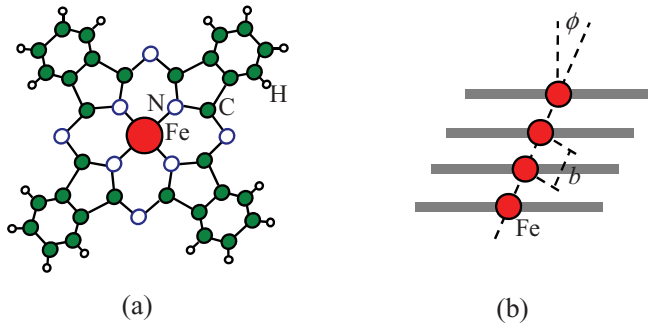


FIG. 1. (Color online) (a) Atomic structure of the Fe phthalocyanine (FePc) molecule; the Fe^{2+} (d^6) ion has D_{4h} symmetry. (b) Chain structure of α -FePc, characterized by a columnar stacking of the planar molecules with separation of $b = 3.78$ Å and a tilt angle $\phi = 26.5^\circ$ with respect to the chain axis.

hysteresis experiments, furthermore, indicated that the easy axis of magnetization is parallel to the molecule plane, i.e., a planar magnetic anisotropy.⁹

Similarly, DFT calculations are still contradictory: recent pseudopotential and full-potential linearized augmented plane-wave (FLAPW) calculations^{16–18} within the GGA support the 3E_g ground state, in which qualitative agreement with experimental observations is obtained for α -FePc,⁹ but the ${}^3A_{2g}$ and ${}^3B_{2g}$ ground states have also been found.^{19–21} Unfortunately, up to now there have not been direct comparisons of the total energies of the various multiplets within a DFT scheme. Thus, determining the ground-state multiplet of the FePc molecule remains unsolved from both the experimental and theoretical points of view.

III. MODEL AND METHOD

To model a single FePc molecule with D_{4h} symmetry, as shown in Fig. 1(a), we adopt a monolayer slab with infinite vacuum on both sides, a large in-plane lattice constant of 27 Å, and the atomic positions given by experiment.²² Calculations were done by the film-FLAPW method^{23,24} and used the GGA²⁵ for exchange correlation. LAPW basis sets with cutoffs of $|\mathbf{k} + \mathbf{G}| \leq 3.6\text{--}4$ a.u.⁻¹ and muffin-tin (MT) sphere radii of 2.3 a.u. for transition metals, 1.2 a.u. for N and C, and 0.8 a.u. for H were used; lattice harmonics with angular momenta up to $\ell = 8$ for Fe, 6 for N and C, and 4 for H are employed to expand the charge and spin densities.

Before presenting our strategy to search for given multiplets, we discuss some aspects of the symmetry in more detail. In D_{4h} symmetry, the nonspherical densities arising from the Fe d orbitals can be expanded into three lattice harmonics: $K_1(\vec{r}) = Y_{20}(\vec{r})$, $K_2(\vec{r}) = Y_{40}(\vec{r})$, and $K_3(\vec{r}) = [Y_{44}(\vec{r}) + Y_{4-4}(\vec{r})]/\sqrt{2}$. Each of the multiplets is a triplet, i.e., four majority and two minority d electrons. The majority nonspherical density is the same for all three multiplets and proportional to $\rho_\uparrow \sim |u_d|^2 [(2\sqrt{5}/7)K_1 - (1/7)K_2 + \sqrt{5/7}K_3]$, where u_d is the radial d orbital. The corresponding minority densities for the various multiplets differ in the coefficients of the lattice harmonics: $\rho_\downarrow(A_{2g}) \sim |u_d|^2 [K_2 + \sqrt{5/7}K_3]$,

$$\rho_\downarrow(B_{2g}) \sim |u_d|^2 [(2\sqrt{5}/7)K_1 - (8/7)K_2], \quad \text{and} \quad \rho_\downarrow(E_g) \sim |u_d|^2 [(-\sqrt{5}/7)K_1 - (3/7)K_2 + \sqrt{5/7}K_3].$$

Starting with initial nonspherical charge and spin densities corresponding to a given multiplet does not necessarily lead to self-consistent results for that multiplet. In fact, using a straight mixing scheme for the spin density, self-consistent calculations are found to converge to the 3E_g solution regardless of the different initial d occupancies, consistent with previous DFT calculations.^{16–18} (Using the “standard” starting density derived from overlapping spherical densities invariably leads to the 3E_g state.)

In self-consistent calculations, the trajectory of the charge/spin density from an initial one is complicated and nonlinear, making definitive statements regarding the self-consistency process difficult. For the present case of FePc D_{4h} symmetry, however, the situation is somewhat simplified since the changes during the self-consistency cycle are mainly governed by the strong hybridization between the minority-spin Fe $d_{xz,yz}$ and neighboring N p_z orbital that form bonding and antibonding states. Since the 3E_g state has one electron in the $d_{xz,yz,\downarrow}$ orbital, the electron occupies only the bonding state, which drives a self-consistent solution to the 3E_g state. By carefully tailoring the mixing scheme, we found that we were able to obtain a ${}^3A_{2g}$ solution (no electron in the $d_{xz,yz,\downarrow}$ orbital). However, we were never able to reach a ${}^3B_{2g}$ solution (two electrons in the $d_{xz,yz,\downarrow}$ orbital), since electrons need to occupy both the bonding and antibonding states, which is generally an unfavorable electronic structure. Thus, in contrast to conventional expectations and practices, the DFT calculations, even with appropriate initial conditions, are *not guaranteed* to treat all multiplets considered and may not—often do not—find the true ground state.

To generalize the DFT method to multiplets with given symmetries, we introduce an appropriate functional with constraint fields:

$$E[\rho(\mathbf{r})] = E_{\text{GGA}}[\rho(\mathbf{r})] + \sum_{mm'} \mu_{m'm}^\alpha (n_{mm'}^\alpha - N_{mm'}^\alpha), \quad (1)$$

where $E_{\text{GGA}}[\rho(\mathbf{r})]$ is the usual total-energy functional in the GGA, $n_{mm'}^\alpha$ is a density matrix of d orbitals of an atom α , and $N_{mm'}^\alpha$ is an occupation number that should be constrained. The $\mu_{m'm}^\alpha$ is a constraint field (Lagrange multiplier parameter)²⁶ that can be viewed as a field to constrain the density matrix, such that the desired multiplet structure is obtained, similar to the external magnetic field in fixed moment calculations. By minimizing Eq. (1), the Kohn-Sham equation can be written as

$$\left[H_{\text{GGA}} + \sum_{mm'} \mu_{m'm}^\alpha \hat{P}_{mm'}^\alpha \right] \Phi_{\mathbf{k},b} = \epsilon \Phi_{\mathbf{k},b}, \quad (2)$$

where $\hat{P}_{mm'}^\alpha$ is a projection operator onto the mm' subspace. The constraint term in the Hamiltonian effectively projects out the chosen irreducible representation for the overall *wave function*. If the constraint fields are zero for a set of $n_{mm'}^\alpha$ (or the constraints are satisfied), the solution obviously is also a solution to the standard unconstrained DFT equations; this situation is again similar to fixed moment calculations where the unconstrained solutions are found when the magnetic

constraint fields are zero (or, equivalently, the minority and majority Fermi levels are equal).

In the LAPW basis, $n_{mm'}^\alpha$ is given by the projection of the wave function onto the $Y_{\ell m}$ subspace²⁷ as

$$n_{mm'}^\alpha = \sum_{\mathbf{k}, b} f_{\mathbf{k}, b} \langle \Phi_{\mathbf{k}, b} | \hat{P}_{mm'}^\alpha | \Phi_{\mathbf{k}, b} \rangle, \quad (3)$$

$$\hat{P}_{mm'}^\alpha = |u_\ell^\alpha Y_{\ell m}\rangle \langle u_\ell^\alpha Y_{\ell m}| + \frac{1}{\langle \dot{u}_\ell^\alpha \dot{u}_\ell^\alpha \rangle} | \dot{u}_\ell^\alpha Y_{\ell m} \rangle \langle \dot{u}_\ell^\alpha Y_{\ell m} |, \quad (4)$$

where \mathbf{k} and b refer to a k point in the Brillouin zone and a band index, respectively. Self-consistent calculations were carried out using the second-variation scheme; i.e., the diagonalization of Eq. (2) was carried out in a basis of the eigenfunctions, $\phi_{\mathbf{k}, b}$, of H_{GGA} . Full self-consistency was achieved for the density matrix as well as the charge and spin densities.

In practice, we specify a set of constraint fields, μ_n^α , along the directions of the eigenvectors of $n_{mm'}^\alpha$ consistent with the site symmetry (e.g., $\mu_{z^2}, \mu_{xz} = \mu_{yz}, \mu_{x^2-y^2}$, and μ_{xy} in the case of D_{4h} symmetry). Then, the $\mu_{mm'}^\alpha$, that are rotated back from the μ_n^α , are introduced in Eq. (2), and the corresponding $n_{mm'}^\alpha$ are determined self-consistently. The total energy is calculated using Eq. (1), with $N_{mm'}^\alpha = n_{mm'}^\alpha$.

Note that the self-consistent solution obtained by first applying constraint fields and then decreasing them to zero need not lead to the same solution as an unconstrained calculation. Although this situation may seem surprising at first, it is rather common and physically significant: Experimentally, there is often a difference in magnetization between field-cooled and zero-field-cooled values, which is of fundamental importance in the physics of spin glasses. Computationally, multiple zero-field (unconstrained) magnetic solutions, including the zero-magnetization/non-magnetic one, often exist; different solutions can be obtained, for example, by (i) using a staggered/uniform magnetic field (the magnitude is then reduced to zero) to pick out AFM/FM order or (ii) varying, for itinerant electron metamagnets²⁸ and high-spin/low-spin ferromagnets, the magnitude of the magnetic field before removing it. Thus, when multiple solutions exist, as is the case for both multiplets and these specific magnetic examples, the application of external constraint fields may be helpful, or sometimes even necessary, in order to obtain the desired unconstrained solution.

IV. RESULTS AND DISCUSSION

The minority-spin occupations, $n_{xz+yz, \downarrow}$, and the total-energy differences, ΔE , with respect to variations of the $\mu_{xz(yz), \downarrow}$ for the single FePc molecule are shown in Figs. 2(a) and 2(b), respectively, when the other μ_n 's are set to zero. Starting from a superposition of spherical atoms and with no constraints, i.e., $\mu_n = 0$ (closed squares in Fig. 2), yields the multiplet structure shown in Fig. 3(a): the singlet d_{xy} in the minority-spin states is fully occupied, and the doublet d_{xz+yz} , located at the top of the valence states, is occupied by one electron, thus corresponding to the 3E_g state. The degeneracy in the doublet d_{xz+yz} occupied by a single electron could be removed by a Jahn-Teller distortion, as pointed out previously.²⁹ We confirmed that the total energy of the system that degrades to a D_{2h} symmetry turns out to be lower by 45 meV/molecule than that with the original D_{4h} symmetry.

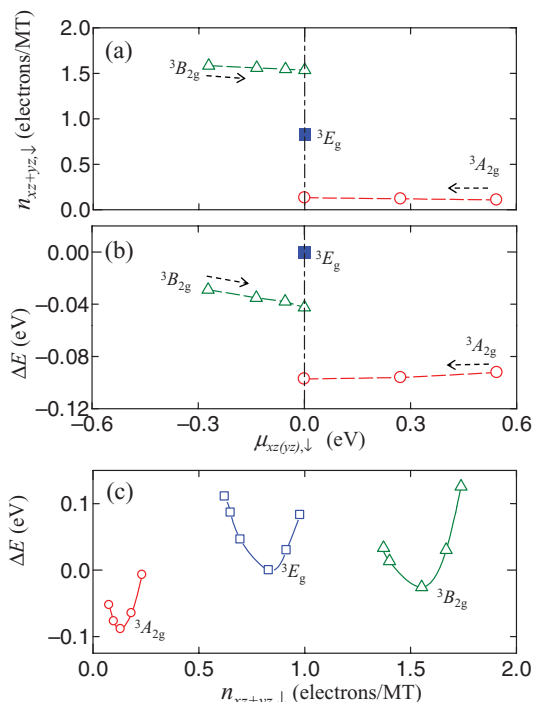


FIG. 2. (Color online) (a) Minority-spin d_{xz+yz} occupations, $n_{xz+yz, \downarrow}$, in the Fe MT sphere and (b) the total-energy difference, ΔE , with respect to the constraint field, $\mu_{xz(yz), \downarrow}$, for the FePc molecule, where the other μ_n 's are set to zero. Closed squares indicate the solution obtained without the constraint field. (c) ΔE as a function of the $n_{xz+yz, \downarrow}$, where the constraint fields, μ_n , are set so as to obtain each multiplet.

When the constraint field $\mu_{xz(yz), \downarrow}$ is introduced in the negative direction (cf. Fig. 2), $n_{xz+yz, \downarrow}$ increases to ~ 1.6 electrons; if $\mu_{xz(yz), \downarrow}$ is decreased to zero (zero constraint field) the system remains in the stationary solution; i.e., the ${}^3B_{2g}$ state is a metastable solution to the standard GGA equations. In this multiplet structure, Fig. 3(b), the doublet d_{xz+yz} in the minority-spin states is fully occupied while the singlet d_{xy} shifts up in energy above the valence top, corresponding to ${}^3B_{2g}$. The total energy is now lower than that of the 3E_g state by 43 meV/molecule.

In contrast, when $\mu_{xz(yz), \downarrow}$ is introduced in the positive direction, $n_{xz+yz, \downarrow}$ decreases almost to zero, at which point the doublet d_{xz+yz} in the minority-spin states shifts up above the top of the valence states and the two singlets d_{xy} and d_{z^2} are fully occupied [Fig. 3(c)]. The total energy of this ${}^3A_{2g}$ configuration is lower than those of the 3E_g and ${}^3B_{2g}$ ones by 97 and 54 meV/molecule, respectively. We thus conclude that the ground state of the single FePc molecule is the ${}^3A_{2g}$ multiplet.

A phase diagram for the multiplets with respect to the $n_{xz+yz, \downarrow}$ is summarized in Fig. 2(c), where the constraint fields μ_n are set so as to obtain each multiplet solution: $\mu_{z^2, \downarrow}$ ($\mu_{xy, \downarrow}$) = 0.03 (−0.03) htr for 3E_g , 0.03 (0.03) htr for ${}^3B_{2g}$, and −0.03 (0.03) htr for ${}^3A_{2g}$. Note that each multiplet solution appears only in a restricted narrow range in $n_{xz+yz, \downarrow}$ space. This behavior rationalizes the observed difficulty of stabilizing, for example, the ${}^3B_{2g}$ solution: During the standard self-consistency process, the occupations of the various Fe

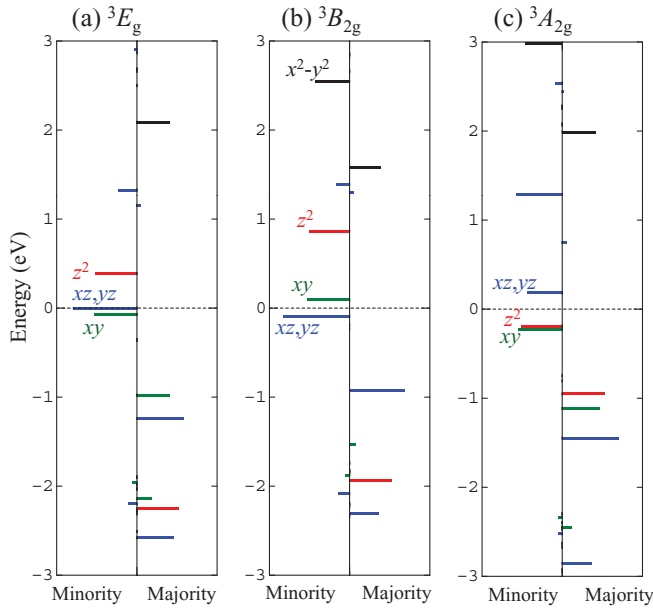


FIG. 3. (Color online) Multiplet structure for (a) 3E_g , (b) ${}^3A_{2g}$, and (c) ${}^3B_{2g}$, obtained as stationary states in self-consistent calculations with zero constraint field ($\mu_n = 0$). Bars (in color) represent weights of d orbitals. Negative and positive energies indicate occupied and unoccupied orbitals, respectively.

(and N) orbitals vary due to hybridization and Fermi filling effects; if these variations are too large (which may be less than ~ 0.1 electron), the solution “jumps” from the initial ${}^3B_{2g}$ manifold to the 3E_g one. However, once the solution is “close enough” to the self-consistent one, the constraint field can be removed and the system will iterate to the metastable solution. Thus, the imposition of the constraints on the density matrix provides an approach that permits the calculation of states that may be difficult to stabilize otherwise, independent of the initial densities. These results indicate that different solutions proposed previously^{16–21} may be sensitive to (or an accidental result of) calculational details.

Next, we consider the electronic structure of α -FePc in the chain structure shown in Fig. 1(b).^{6,7} Note that although the columnar stacking breaks the D_{4h} symmetry at the Fe position the constraint fields, as done previously, can still be imposed. No stationary ($\mu_n = 0$) solutions for the ${}^3B_{2g}$ and ${}^3A_{2g}$ states are found, and the ground state is determined to be 3E_g ; the total energy is now lower than those of the ${}^3B_{2g}$ and ${}^3A_{2g}$ states by about 200 and 100 meV/molecule, respectively, when compared to the lowest energies in the constraint fields.

The calculated band structure along the chain axis and the partial density of states (DOS) of the Fe d orbitals for the 3E_g state are shown in Fig. 4. Due to hybridization between the adjacent molecules along the chain axis, the d_{xz+yz} and d_{z^2} orbitals have large dispersion along the chain axis, and a small energy gap (0.17 eV) in the minority-spin d_{xz+yz} bands appears, indicating semiconducting behavior. As seen in the DOS, the hybridization pushes the bonding d_{xz+yz} bands down to a lower energy below the top of the valence band, which causes the ground state to be the 3E_g one.

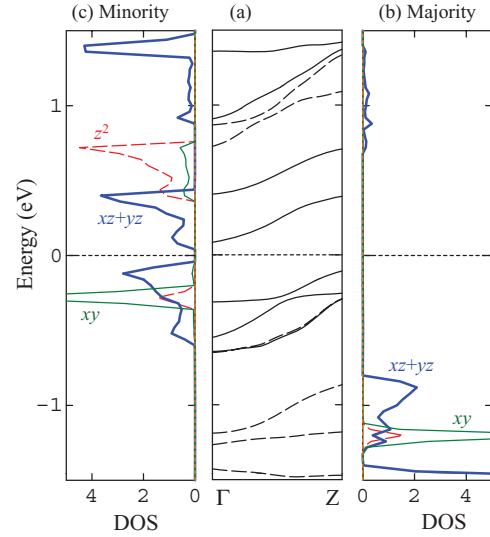


FIG. 4. (Color online) (a) Calculated band structure along the chain axis: solid (dashed) lines represent the majority (minority) bands. (b) Majority- and (c) minority-spin partial density of states of d orbitals in the 3E_g state. Thick solid (blue), thin solid (green), thin dashed (red), and thin dotted (orange) lines represent d_{xz+yz} , d_{xy} , d_{z^2} , and $d_{x^2+y^2}$ states, respectively.

We also carried out magnetic anisotropy calculations for the chain structure, using the second variational spin-orbit coupling method and the force theorem,^{30–32} where the magnetic anisotropy energy, E_{MA} , is obtained as the energy eigenvalue difference for the magnetization oriented along the in-plane and out-of-plane directions with respect to the molecule plane. The calculations demonstrate that E_{MA} has a large negative value of 0.6 meV/molecule, indicating that the magnetization energetically favors pointing in the planar direction and a large orbital moment of $0.14 \mu_B$ is induced, in qualitative agreement with recent XMCD experiments.⁹ In addition, the calculated hyperfine field due to the Fermi contact term is found to have a positive value of 13.4 T, i.e., to be parallel to the magnetic moment, due to a large positive contribution from the valence s -like electrons. (The quantitative discrepancy with the Mössbauer experiments⁸ may be attributed to the underestimation of the orbital moment in the calculation.)

V. SUMMARY

In summary, we have generalized the DFT total-energy calculations to treat different multiplets in a ligand field by incorporating a density-matrix constraint to control the occupation numbers of electrons in d orbitals. We have applied this approach to solve a long-standing question regarding the ground state of FePc: We find three stationary states, 3E_g , ${}^3A_{2g}$, and ${}^3B_{2g}$, of the Fe^{2+} ion in the single FePc molecule, with total-energy calculations demonstrating that the ground state is the ${}^3A_{2g}$ configuration. The columnar stacking of the FePc molecules in the α -FePc changes the ground state to 3E_g , due to the hybridization between adjacent molecules along the chain axis. The magnetic anisotropy calculations indicate that the magnetization is preferentially

in-plane and large orbital moments are induced, in agreement with the recent XMCD experiments.

ACKNOWLEDGMENTS

We thank Prof. Jae Il Lee for fruitful discussions. Work at Mie University was supported by the Young Researcher Overseas Visits Program for Vitalizing Brain Circulation

(Grant No. R2214) from the Japan Society for the Promotion of Science, and computations were partially performed at the Institute for Solid State Physics, University of Tokyo. Work at Northwestern University was supported by the U.S. Department of Energy (Grant No. DE-FG02-88ER45372) and at the University of Wisconsin-Milwaukee by the National Science Foundation (Grants No. DMR-0706359 and No. DMR-1105839).

*kohji@phen.mie-u.ac.jp

¹U. von Barth, *Phys. Rev. A* **20**, 1693 (1979); M. Weinert, R. E. Watson, and G. W. Fernando, *ibid.* **66**, 032508 (2002), and references therein.

²A. Szabo and N. S. Ostlund, *Modern Quantum Chemistry* (McGraw-Hill, New York, 1982).

³K. Ogasawara, T. Ishii, I. Tanaka, and H. Adachi, *Phys. Rev. B* **61**, 143 (2000).

⁴*Phthalocyanines, Properties and Applications*, edited by C. C. Leznoff and A. B. P. Lever (VCH, New York, 1996).

⁵S. E. Harrison and K. H. Ludewing, *J. Chem. Phys.* **45**, 343 (1966).

⁶C. Ercolani, C. Neri, and P. Porta, *Inorg. Chim. Acta* **1**, 415 (1967).

⁷M. Evangelisti, J. Bartolome, L. J. de Jongh, and G. Filoti, *Phys. Rev. B* **66**, 144410 (2002).

⁸G. Filoti, M. D. Kuz'min, and J. Bartolomé, *Phys. Rev. B* **74**, 134420 (2006).

⁹J. Bartolomé, F. Bartolomé, L. M. García, G. Filoti, T. Gredig, C. N. Colesniuc, I. K. Schuller, and J. C. Cezar, *Phys. Rev. B* **81**, 195405 (2010).

¹⁰L. Klemm and W. Klemm, *J. Prakt. Chem.* **143**, 82 (1935).

¹¹A. B. P. Lever, *J. Chem. Soc.* **1965**, 1821 (1965).

¹²B. W. Dale, R. J. P. Williams, C. E. Johnson, and T. L. Thorp, *J. Chem. Phys.* **49**, 3441 (1968).

¹³C. G. Barraclough, R. L. Martin, S. Mitra, and R. C. Sherwood, *J. Chem. Phys.* **53**, 1643 (1970).

¹⁴M. J. Stillman and A. J. Thomson, *J. Chem. Soc., Faraday Trans. 2* **70**, 790 (1974).

¹⁵P. Coppens, L. Li, and N. J. Zhu, *J. Am. Chem. Soc.* **105**, 6173 (1983).

¹⁶B. Bialek, I. G. Kim, and J. I. Lee, *Surf. Sci.* **526**, 367 (2003).

¹⁷J. Wang, Y. Shi, J. Cao, and R. Wu, *Appl. Phys. Lett.* **94**, 122502 (2009).

¹⁸M. D. Kuz'min, R. Hayn, and V. Oison, *Phys. Rev. B* **79**, 024413 (2009).

¹⁹M.-S. Liao and S. Scheiner, *J. Chem. Phys.* **114**, 9780 (2001).

²⁰M. Sumimoto, Y. Kawashima, K. Hori, and H. Fujimoto, *Spectrochim. Acta A* **71**, 286 (2008).

²¹P. A. Reynolds and B. N. Figgis, *Inorg. Chem.* **30**, 2294 (1991).

²²J. F. Kirner, W. Dow, and W. R. Sheidt, *Inorg. Chem.* **15**, 1685 (1976).

²³E. Wimmer, H. Krakauer, M. Weinert, and A. J. Freeman, *Phys. Rev. B* **24**, 864 (1981).

²⁴M. Weinert, E. Wimmer, and A. J. Freeman, *Phys. Rev. B* **26**, 4571 (1982).

²⁵J. P. Perdew, K. Burke, and M. Ernzerhof, *Phys. Rev. Lett.* **77**, 3865 (1996).

²⁶P. H. Dederichs, S. Blügel, R. Zeller, and H. Akai, *Phys. Rev. Lett.* **53**, 2512 (1984).

²⁷A. B. Shick, A. I. Liechtenstein, and W. E. Pickett, *Phys. Rev. B* **60**, 10763 (1999).

²⁸S. Khmelevskiy, P. Mohn, J. Redinger, and M. Weinert, *Phys. Rev. Lett.* **94**, 146403 (2005).

²⁹P. S. Miedema, S. Stepanow, P. Gambardella, and F. M. F. De Groot, *J. Phys.: Conf. Ser.* **190**, 012143 (2009).

³⁰C. Li, A. J. Freeman, H. J. F. Jansen, and C. L. Fu, *Phys. Rev. B* **42**, 5433 (1990).

³¹M. Weinert, R. E. Watson, and J. W. Davenport, *Phys. Rev. B* **32**, 2115 (1985).

³²G. H. O. Daalderop, P. J. Kelly, and M. F. H. Schuurmans, *Phys. Rev. B* **41**, 11919 (1990).